

**METAGENOME ANALYSIS OF AN ENRICHMENT CULTURE
THAT DEGRADES THE 3-NITRO-1,2,4-TRIAZOL-5-ONE (NTO)
EXPLOSIVE**

A Thesis
Presented to
The Academic Faculty

by

Doyoung Park

In Partial Fulfillment
of the Requirements for the Degree
Master of Environmental Engineering in the
School of Civil and Environmental Engineering

Georgia Institute of Technology
August 2020

COPYRIGHT © 2020 BY DOYOUNG PARK

**METAGENOME ANALYSIS OF AN ENRICHMENT CULTURE
THAT DEGRADES THE 3-NITRO-1,2,4-TRIAZOL-5-ONE (NTO)
EXPLOSIVE**

Approved by:

Dr. Konstantinos T. Konstantinidis, Advisor
School of Civil and Environmental Engineering
Georgia Institute of Technology

Dr. Jim C. Spain
School of Biology
University of West Florida

Dr. Spyros G. Pavlostathis
School of Civil and Environmental Engineering
Georgia Institute of Technology

Date Approved: December, 2020

ACKNOWLEDGEMENTS

First, I have to thank my research supervisor, Professor Konstantinos T. Konstantinidis: he gave me insightful and constructive comments and encouragement throughout my graduate studies. Without his guidance and persistent help, this thesis would not have been possible. Also, I am deeply grateful to Professor Jim C. Spain for sharing expertise. His valuable inputs during the project always made me motivated towards studying. I also appreciate the feedback offered by Professor Spyros G. Pavlostathis. I would like to thank all the members of Kostas' lab group including Dr. Smruthi Karthikeyan and Dr. Minjae Kim for their feedback, cooperation, and of course friendship. Last but not the least, I am grateful to my families who supported me spiritually.

TABLE OF CONTENTS

ACKNOWLEDGEMENTS	i
LIST OF TABLES	iii
LIST OF FIGURES	iv
SUMMARY	v
CHAPTER 1. Introduction	1
1.1 Insensitive munitions compound 3-Nitro-1,2,4-triazole-5-one (NTO) and its reduced product, 3-amino-1,2,4-triazol-5-one (ATO)	1
1.2 Biodegradation and environmental implications of NTO and ATO	2
1.3 Objectives of this study	3
CHAPTER 2. Materials and Methods	4
2.1 Development of enrichment cultures for metagenome analysis	4
2.1.1 NTO-reduction enrichment culture	4
2.1.2 ATO-mineralization enrichment culture	4
2.2 DNA extraction and sequencing	6
2.3 Bioinformatics analysis of metagenomic reads	8
2.3.1 Quality control and assembly	8
2.3.2 Sequence coverage	9
2.3.3 16S rRNA gene fragment analysis	11
2.3.4 Population genome binning and determining MAG abundance	12
2.3.5 Finding rRNA genes of MAGs	13
2.3.6 Functional annotation of MAGs	13
2.3.7 Flux balanced analysis (FBA)	15
CHAPTER 3. Results	16
3.1 Consortium composition based on 16S rRNA gene sequence fragments	16
3.2 Recovery of metagenome-assembled genomes (MAGs)	18
3.3 NTO consortium	20
3.4 Potential degradation of NTO in these MAGs	21
3.5 Original ATO consortia	25
3.6 Derived ATO consortia	27
3.7 Prediction of functional dependence and interactions among members of the ATO consortium	29
CHAPTER 4. Discussion	33
CHAPTER 5. Conclusions	41
APPENDIX A. Supporting Information	42

LIST OF TABLES

Table 1	Statistics of the metagenomes used in this study	10
Table 2	Summary statistics of the MAGs reported by our study	19
Table 3	Candidate nitroreductases for NTO reduction to ATO and their experimentally verified best match homolog	22
Table 4	Candidate cyclic amide hydrolase for ATO degradation and their best match homolog	40
Table S1	<i>Geobacter</i> MAG cytochromes based on cytochrome annotation	42
Table S2	Proposed <i>Geobacter</i> MAG EET (extracellular electron transfer system) based on cytochrome annotation	42
Table S3	The composition of ATO minimal medium used in FBA.	43

LIST OF FIGURES

Figure 1	Microbial community coverage by sequencing and complexity as assessed by Nonpareil	9
Figure 2	Relative abundance of 16S rRNA V4 region gene-based OTUs at the genus level	17
Figure 3	Composition of the NTO-reducing and ATO-mineralizing microbial consortia.	21, 27, 29
Figure 4	Prediction of functional dependencies and exchange of metabolites among MAGs of the ATO consortium	30, 32
Figure 5	Proposed NTO degradation pathways	34
Figure S1	Development of ATO enrichment cultures	44

SUMMARY

3-Nitro-1,2,4-triazol-5-one (NTO) is an essential component of the newly introduced insensitive high explosive (IHE) compounds as it has several advantages, namely low shock sensitivity and easy synthesis. With increasing use by the military, it is important to understand the fate of NTO in the environment and its biodegradation. Previous studies have shown that NTO is at first reduced to 3-amino-1,2,4-triazol-5-one (ATO) under anaerobic conditions and, subsequently, ATO is fully mineralized aerobically to NH_4^+ , CO_2 , and N_2 by microbes. To provide new insights into the degradation process, we performed shotgun metagenome sequencing of the NTO-degrading consortium (enrichment culture) and two sets of ATO-degrading enrichment cultures; one is original ATO cultures developed from a dilution to extinction experiment and the other is the ATO cultures derived from the original ATO cultures by physically disruption and additional dilution to extinction in order to break the extracellular matrix between different microbial species and further reduce the diversity of the consortium. Two metagenome-assembled genomes (MAGs) were recovered from the NTO dataset that made up >95% of the total culture and carried putative nitroreductases that might be involved in NTO reduction. In addition, the presence of extracellular electron transfer systems in the most abundant MAG (a *Geobacter* sp., making up 89.3% of the total) suggested that these systems might also be involved in NTO reduction. The ATO metagenomes revealed seven MAGs that were consistently observed and -more or less- evenly distributed in the three consortia. Functional annotation of these MAGs and flux balanced analysis revealed several amino acids auxotrophies in different species and metabolite exchange between members of the

consortium, respectively, which probably underlie the interactions among the several MAGs during ATO mineralization. Collectively, the findings reported here provide the genetic basis for NTO biodegradation and have implications for future NTO bioremediation efforts.

CHAPTER 1. INTRODUCTION

1.1 Insensitive munitions compound 3-Nitro-1,2,4-triazole-5-one (NTO) and its reduced product, 3-amino-1,2,4-triazol-5-one (ATO)

In addition to 2,4-dinitroanisole (DNAN), 3-Nitro-1,2,4-triazol-5-one (NTO) is an essential element of the newly introduced insensitive high explosive (IHEs) compounds[3, 4]. Recently, NTO has attracted attention because it is an alternative to traditional munitions such as trinitrotoluene (TNT), and hexahydro-1,3,5-trinitro-1,3,5-triazine (RDX) due to possessing several advantages. Most notably, NTO has low shock sensitivity and is easily synthesized, which makes it appropriate for munitions[5]. As NTO is increasingly used by the military, its environmental impact and fate should be better understood. Compared to other explosive compounds such as TNT or RDX, NTO has a higher solubility, so it readily dissolves in rainwater and gets transported through the soil as evidenced by the low sorption of NTO based on Br⁻ tracer tests and laboratory drip tests [4, 6] to potentially reach groundwater.

1.2 Biodegradation and environmental implications of NTO and ATO

An initial study of NTO biodegradation showed that NTO can be reduced to ATO by the rat liver cytochrome P450 enzyme[7]. NTO can also be degraded by a strain of *Bacillus licheniformis*, although in this case a relatively high quantity of co-substrate (> 15 g l⁻¹ of glucose) was required[8]. Over the past years, several studies have shown that NTO can be fully mineralized to CO₂, NH₄⁺, and N₂ by microbial consortia in two steps^[9-11]. First, NTO is anaerobically reduced to 3-amino-1,2,4-triazol-5-one (ATO) via 3-hydroxyamino-1,2,4-triazol-5-one (HTO)[9]. Subsequently, ATO is completely degraded to CO₂, NH₄⁺, and N₂ under aerobic conditions by a soil-derived enrichment culture[10, 11]. Notably, the genetic determinants of both pathways (i.e., anaerobic transformation of NTO to ATO and aerobic ATO mineralization) are still unknown limiting bioremediation applications and monitoring of the biodegradation process with molecular tools such as PCR assays.

Madeira et al. studied the community responsible for ATO mineralization by 16S rRNA gene amplicon sequencing and qPCR of ATO enrichment cultures[11]. Nine phylogenetic groups were present in the consortium after the 10⁻⁷ (v/v) dilution to extinction and more stringent dilution series, 10⁻³ (v/v), from the 55th enrichment culture transfer. The nine phylogroups included *Terrimonas* spp., *Ramlibacter-related* spp., *Mesorhizobium* spp., *Hydrogenophaga* spp., *Ralstonia* spp., *Pseudomonas* spp., *Ectothiorhodospiraceae* spp., *Sphingopyxis* spp., and *Taonella* spp, and each phylogroup seemed to be evenly abundant in the consortium. However, it remained unclear whether all phylogroups were necessary for ATO degradation and what were the genetic determinants of ATO biodegradation. Further, the 16S rRNA gene sequence often does not provide

resolution to the species level[12], and thus distinct populations may carry identical or nearly identical 16S rRNA gene sequences and be grouped under the same phylotype. Therefore, to better understand the organisms and genes involved in ATO biodegradation, we performed metagenome sequencing of the derived consortia after dilution to extinction and additional manipulations to reduce culture complexity.

1.3 Objectives of this study

The main objective of this study was to understand which organisms are involved in the mineralization of NTO into inorganic compounds via an ATO intermediate and which metabolic genes are involved in NTO/ATO biodegradation. Metagenomic sequencing was applied to an NTO enrichment culture that was derived from an anaerobic sludge reactor of a wastewater treatment plant as well as to an ATO enrichment culture derived from gortner garden soil collected on the University of Minnesota campus, which was previously described by 16S rRNA gene amplicon sequencing[11]. The microbial consortia were examined at both the 16S rRNA gene level based on metagenome reads carrying the V4 region and by the metagenome-assembled population genomes (MAGs). We also report on the candidate genes that were recovered in the MAGs and their possible involvement in NTO and ATO degradation.

CHAPTER 2. MATERIALS AND METHODS

2.1 Development of enrichment cultures for metagenome analysis

2.1.1 NTO-reduction enrichment culture

The enrichment provided by Dr. Jim Field group, University of Arizona, AZ was developed as follows. An NTO-reducing enrichment culture was developed from a sample collected from an anaerobic digester sludge reactor of the Tres Rios Wastewater Reclamation Facility in Tucson, Arizona. One gram of the sludge was diluted in 1L of mineral medium containing (in mg L⁻¹): K₂HPO₄ (250), CaCl₂·2H₂O (10), MgSO₄·7H₂O (100), NH₄Cl (20), NaHCO₃ (4,000) with the trace elements. Sodium acetate (2,000 μM) was used as a carbon source and NTO was added to the medium at a concentration of 500 μM. To establish anaerobic conditions, all serum bottles were sealed with rubber stoppers, and the headspace of all NTO enrichment culture was flushed with 80% N₂ and 20% CO₂ after the medium. After two dilution-to-extinction attempts from the 54th transfer of the consortium (10⁻⁸ and 10⁻⁵ (v/v) dilution each), the consortium that showed NTO reduction was analyzed in this study.

2.1.2 ATO-mineralization enrichment culture

The ATO enrichment culture provided by Dr. Jim Spain group, University of West Florida, FL was developed as follows. An ATO enrichment culture for the first metagenome sequencing analysis was prepared from a 10⁻⁷ (v/v) diluted culture using the 55th transfer of the consortium from Madeira *et al.*[11] as inoculum . Briefly, this enrichment culture was developed from 10 g L⁻¹ of the Gortner Garden soil in 40 mL

mineral medium. The enrichment culture was grown aerobically with shaking (130 rpm) in 30 °C and transferred to fresh mineral media once all ATO was degraded. After 12 transfers, the enrichment was transferred to the medium without yeast extract, that is, ATO as the sole carbon and nitrogen sources. A dilution-to-extinction (10^{-7} v/v) was performed from the 55th transfer to select for a reduced diversity community and identify key members of ATO biodegradation. To maintain this culture, it was transferred multiple times via weekly 10% dilution, and three actively grown derived cultures, A, B, and C (biological replicates), were used for the original ATO metagenome sequencing analysis.

Metagenome sequencing of replicate cultures A, B, and C revealed a relatively complex consortium (for the number of transfers and the dilution to extinction effort) composed of eight species (see below). In an attempt to further reduce the diversity of this consortium, one of the enrichment cultures (culture B) was amended with 3mm glass beads and 1.0 mM NaCl or 3.0 mM EDTA, which are efficient at extracting extracellular matrix[13], and vortexed to physically and chemically disrupt any extracellular matrix between microbial cells and subsequently force those cells that are not essential for the biodegradation to extinction. Another two dilution to extinctions were subsequently performed with the two samples transferred weekly from the culture A and B, and the two vortexed culture B-derived cultures. The highest dilution that showed ATO degradation activity was the 10^{-8} tube for all 4 samples. The cultures transferred from the four 10^{-8} cultures were, A2, B2, B2_NaCl, and B2_EDTA, were used for the derived ATO metagenome sequencing analysis. ATO concentrations were monitored with an Agilent 1200 series HPLC (Agilent, Santa Clara, CA) and a Syringe 4 μ Polar-RP 80A column

(150 X 4.6mm) for all cultures. The mobile phase used was 100% water at a flow rate of 1.0 mL/minute. Absorbance was monitored at 210 nm.

2.2 DNA extraction and sequencing

For the NTO enrichment culture sequencing, 25 mL of three replicate cultures was filtered through a Sterivex-GP Pressure filter to collect biomass (0.22 μm pore size, Millipore Sigma, Burlington, MA). The filter was stored at $-80\text{ }^{\circ}\text{C}$ until DNA was extracted. DNA was extracted by using a phenol-chloroform extraction as previously described[14] with minor modifications. one-fourth of the filter was placed in a microcentrifuge tube with lysis buffer (50 mM Tris-HCl pH 8.3, 40 mM EDTA, and 0.75 M sucrose), and the cells were disrupted with a mini bead beater 24 (BioSpec Products, Bartlesville, OK) at maximum speed twice for one minute each with icing in between. DNA samples from technical replicates were pooled for sequencing.

For the ATO enrichment culture sequencing, 100 mL of culture was centrifuged for collection of biomass and the resulting pellet washed with 1.75 ml phosphate buffer (0.02 M, pH 7.0). DNA was extracted with a GeneJET Genomic DNA Purification Kit (Thermo Fisher Scientific, Waltham, MA) or QIAamp DNA Micro Kit (QIAGEN, Hilden, Germany) according to the manufacturer's protocols.

DNA sequencing libraries were prepared using Illumina's Nextera XT DNA library prep kit according to the manufacturer's protocol except the protocol was terminated after isolation of cleaned double-stranded libraries. Library concentrations were measured using a Qubit HS DNA assay and Qubit 2.0 fluorometer (Thermo Fisher Scientific). To determine

library insert sizes, library samples were run on a 2100 Bioanalyzer instrument (Agilent) using the High Sensitivity DNA chip. The NTO metagenomic library was sequenced on an Illumina MiSEQ for 500 cycles (2 x 250-bp paired-end) and the original and derived ATO metagenomes were sequenced on an Illumina HiSEQ 2500 and NextSEQ 500 instrument for 300 cycles (2 x 150-bp paired-end), respectively, in the Georgia Institute of Technology Molecular Evolution Core facility. Adapter trimming and de-multiplexing were carried out on each instrument.

2.3 Bioinformatics analysis of metagenomic reads

2.3.1 Quality control and assembly

Illumina sequence reads of the NTO and ATO metagenomes were trimmed and read quality was assessed by using FaQCs with a minimum cut-off of Q=30 (99.9% accuracy per base-position) with length of 50 bp[15]. The trimmed reads were assembled using IDBA-UD v 1.1.1[16] with default options for each metagenome; in-house scripts of the enveomics collection[17] were used to prepare the data and process the resulting assembly files. A co-assembly of the corresponding metagenomes was tried to increase recovery of the genomes.

2.3.2 Sequence coverage

To assess the sequencing coverage of the sampled consortia, i.e., what percent of the total community was sequenced, Nonpareil v 3.303 with default settings and the alignment algorithm[18] was used for all metagenome samples including the NTO, the original ATO, and derived ATO metagenomes. The underlying statistics are summarized in Table 1 and the results of Nonpareil in Figure 1.

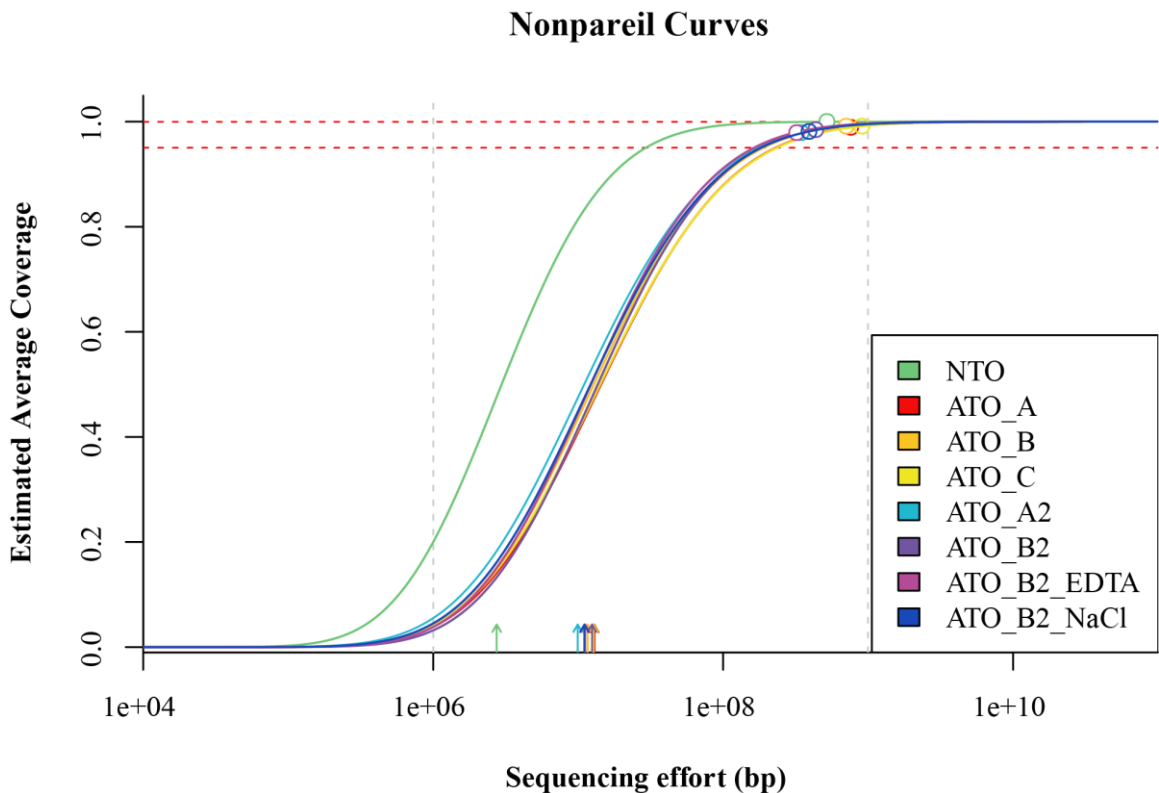


Figure 1 Microbial community coverage by sequencing and complexity as assessed by Nonpareil. Nonpareil estimates of dataset complexity and sequencing effort needed to achieve the desirable coverage level based on read redundancy are shown. Circles represent estimated coverage; the dashed lines represent 95% and 99% of coverage, respectively. The arrows represent the sequencing effort required for achieving 50% of coverage.

Table 1 Statistics of the metagenomes used in this study

Metageno-me characteristics	NTO	ATO				ATO2				
		A	B	C	Co-assembly	A2	B2	B2_EDTA	B2_NaCl	Co-assembly
Trimming results										
Average raw length (bp)	204.3	142.2	146.8	138.2		150.4	149.9	149.7	149.6	
Raw reads (million reads)	6.5	11.1	10.1	13.5		5.5	6.5	4.8	6.0	
Average trimmed length (bp)	177.6	142.1	146.0	138.9		142.5	143.9	143.6	143.2	
Trimmed reads (million reads)	5.7	10.6	9.6	12.9		5.0	6.1	4.3	5.5	
Assembly results										
N50 (bp)	27244	95703	45199	99411	146854	37588	46267	36551	36120	96898
Sequences	652	3726	5510	864	2491	2909	2036	4333	5152	3902
Total length (Mb)	7.6	36.7	36.7	33.8	39.6	28.1	28.4	27.0	29.5	33.3
V4 region fragments	963	256	281	435						

2.3.3 16S rRNA gene fragment analysis

Extraction of the V4 region of the 16S rRNA (16S) genes from metagenomic reads followed the procedure described in Johnston *et al.*[19] with minor modifications. Specifically, to obtain a reference V4 region database for searching against the metagenomic reads, 16S V4 region primers[20] were aligned *in silico* against the GreenGenes 16S full-length database (May 2013 version) by running blastn[21]. Then, the sequences which matched both the forward and reverse primers with over 90% nucleotide identity were selected. The selected sequences were trimmed to include only the V4 region (not upstream or downstream sequences), and the curated V4 region sequences were used as a reference database. Subsequently, metagenome reads were searched against the curated V4 region database by using blastn with -task megablast, -word_size 19 options[21, 22]. The best match for each read was identified when the read had better than 70% nucleotide sequence identity to the database sequence and was trimmed as described above to include only the V4 region. Subsequently, the trimmed reads were used as input for QIIME2 and analyzed using the *de novo* clustering method[23]. The reads were dereplicated using the vsearch dereplicate-sequences command and clustered in Operational Taxonomic Units (OTUs) based on the 97% of sequence similarity with the cluster-features-de-novo --p-perc-identity 0.97[24] command. Taxonomic annotation of 97% OTUs was performed with the feature-classifier plugin by using SILVA database[25] as implemented in QIIME 2 (Silva_132_97_16S.qza file).

2.3.4 *Population genome binning and determining MAG abundance*

Assembled contigs longer than 500 bp were used for binning with MaxBin 2.0 with default options[26]. To taxonomically classify MAGs (i.e., identify the closest named taxon), the MiGA webservice was used with the NCBI Prokaryote genome database option[27].

The relative abundance of the MAGs in each metagenomic sample was calculated by multiplying the genome size of the MAGs and the average sequence coverage of the MAGs obtained by read-recruitment plots[17], and dividing by the total number of the trimmed bases in the corresponding metagenome. The 80% central truncated average of sequencing depth (TAD80) using mapped reads with identity > 95% to the reference MAG (species-level) was used for the average sequence coverage. TAD80 removes the 10% highest and lowest coverage outliers from the relative abundance estimate in order to avoid the effects of -for example- highly conserved genes (e.g., 16S) that recruit reads from non-target populations.

2.3.5 Finding rRNA genes of MAGs

rRNA genes in the MAGs were identified with blast searches against the RDP database release 11.5[28]. The sequences of the MAGs were aligned against the RDP database by using blastn with -max_target_seqs 4 option[21]. The blast results were filtered by 97% nucleotide identity and the best matches were selected. To recover 16S rRNA genes of the MAG sequences that did not include a 16S rRNA gene, we attempted to link the MAGs and their corresponding 16S rRNA genes as described in Karthikeyan *et al.*[29] with minor modifications. Briefly, 16S V4 OTUs from metagenomes were utilized to identify which 16S V4 OTUs correlated strongly to the abundance of the MAGs and provide a taxonomy similar to that produced using the MiGA webserver based on the genome-average amino-acid identity (AAI) approach. The correlated 16S V4 OTUs sequences were subsequently identified on a contig in the assembled metagenome (100% nucleotide sequence identity and 100% query cover). The matched contigs were further analyzed by RNAmmer1.2[30] to recover full length or longer 16S rRNA sequences of the MAGs (ie extend the sequence beyond the V4 region).

2.3.6 Functional annotation of MAGs

Predicted protein-coding open reading frame (ORF) sequences were obtained from MiGA[27]. To identify any homologs of nitroreductase, which might be responsible for NTO reduction, ORFs were searched against a nitroreductase gene database obtained from UniprotKB by searching with the keywords “nitroreductase existence:"evidence at protein level”[31]. Protein sequences were aligned using Diamond v 0.9.22.123 with the blastp option[32]. A minimum cut-off for a match of 30% identity and alignment length over 25

amino acids was used for these searches. To further understand the potential mechanism of electron transfer in the most abundant genome, the extracellular electron transfer systems (EET) of NTO_MAG1 were identified as described in Ishii *et al.* with minor modifications[33]. To identify ORFs encoding a covalent heme-binding motif of c-type cytochrome, the ORFs were analyzed using the FIMO tool v 5.1.1 in MEME suite [34], and ORFs that contained at least two heme motifs were selected as EET genes. The selected ORFs were assigned into the c-type cytochrome family ID[35] based on the best blast match with a minimum cutoff for a match of 70% query coverage, 70% amino acid identity, and 10^{-6} e-value (query cover = alignment length/query gene length \times 100%).

For ATO metagenomes, a curated database for cyclic amide hydrolases acting on carbon-nitrogen bonds other than a peptide bond was obtained from the UniProtKB database by searching EC number or gene name with the corresponding keywords. The keywords used were cyanuric acid amidohydrolase, searched with “ec:3.5.2.15 AND reviewed:yes”; hydantoinase/dihydropyrimidinase, with “ec:3.5.2.2 AND reviewed:yes”; barbiturase (EC 3.5.2.1) with “name:barbiturase AND reviewed:yes”; Allantoinase (EC 3.5.2.5), with “name:allantoinase AND reviewed:yes”; B-Lactamase (EC 3.5.2.6), with “ec:3.5.2.6 AND reviewed:yes”; creatinase (EC 3.5.2.10) with “ec:3.5.2.10 AND reviewed:yes”, an dihydroortase, with “ec:3.5.2.3 AND reviewed:yes”). Mouse, rat, plant and human gene homologs were removed manually.

To identify overall metabolic pathways of the MAGs and evaluate them for amino acid auxotrophies, functional annotation was done by using RASTtk v 2.0[36]. Draft metabolic models of each of the MAGs was established by using ModelSEED v 2.5.1 without the no gap-filling option[37] and KAAS v 2.1[38]. Amino acid auxotrophies were

determined based on the presence/absence of genes involved in bacterial amino acid biosynthesis pathways in the MetaCyc database[39].

2.3.7 Flux balanced analysis (FBA)

To assess potential interactions among members of the ATO consortium, a metabolic model for each MAG was reconstructed, and FBA of the models was performed using the Kbase platform[40]. Reconstruction of compartmentalized models and additional FBA was performed as described in Henry *et al.*[41]. Briefly, to mimic the ATO enrichment culture, the mineral medium used in ATO enrichment experiments was used. Since it was not possible to know the exact compounds used as C and N source by each population of the ATO consortium, and which genes were responsible for ATO degradation, the NH_4^+ was used as the N source in the FBA model. Both C-source free mineral media, which assumes (inorganic) carbon fixation, and lactate amended mineral medium were used to gapfill the model and simulate FBA (Supporting Information Table S4). Specifically, the compartmentalized model was selected from the several models provided by Henry *et al.*[41] to see the interaction of metabolites between each genome. The coefficients of the biomass in the merged pre-gapfilled model were adjusted based on the relative abundance of the ATO_B culture by using the python script in Kbase according to Henry *et al.* [41].

CHAPTER 3. RESULTS

3.1 Consortium composition based on 16S rRNA gene sequence fragments

Coverage of all sampled consortia by metagenomic sequencing as assessed by Nonpareil was in the range of 95.54% to 98.29% indicating that nearly the whole consortium was covered by sequencing, and only a few, rare members may not be well represented in our sequencing results (Figure 1). A total of 93 OTUs were found in the NTO metagenome by analyzing the 16S rRNA gene V4 region, but only 6 OTUs showed higher than 1% of the total relative abundance (Figure 2A). At the genus level, four OTUs assigned to the *Geobacter* genus were predominant showing a cumulative 71.4% of relative abundance. The second most dominant taxon was assignable to the *Betaproteobacteriales* order consisting of two OTUs and 10.5% of the relative abundance of the sample.

All three original ATO samples (A, B, and C) were derived from the ATO biodegradation[11] culture that was enriched from a soil inoculum and transferred over 55 times since. Therefore, it was of interest to determine whether the three cultures had the same microbial composition. A total of 14 OTUs were found in the three enrichment cultures (Figure 2B) based on 16S rRNA gene fragments recovered in the metagenomes. Among these, 7 OTUs were shared and predominant in all three samples showing high cumulative relative abundance: 98.9% in culture A, 98.8% in culture B, and 99.3% in culture C. However, the relative abundance of these individual OTUs was not similar among the three consortia with the most dominant OTU being different in each sample. For example, the relative abundance of an OTU assigned to the *Xanthobacteraceae* family made up 53.4% of the total in culture A while showing a relatively low abundance (15.2%

and 8.0%) in the other two cultures. The most abundant OTU in culture B was assigned to the *Thioalkalispira* genus (46.5%) while this OTU showed low relative abundance (6.4% and 14.0%) in the other two samples. For culture C, the most abundant OTU (64.4%) was assigned to the *Betaproteobacteriales* order. Besides these three dominant OTUs, the distribution of the other four OTUs assigned to the *Hyphomicrobiaceae* family, *Chitinophagaceae* family, *Taonella* genus, and *Sphingopyxis* genus were relatively similar among the three consortia.

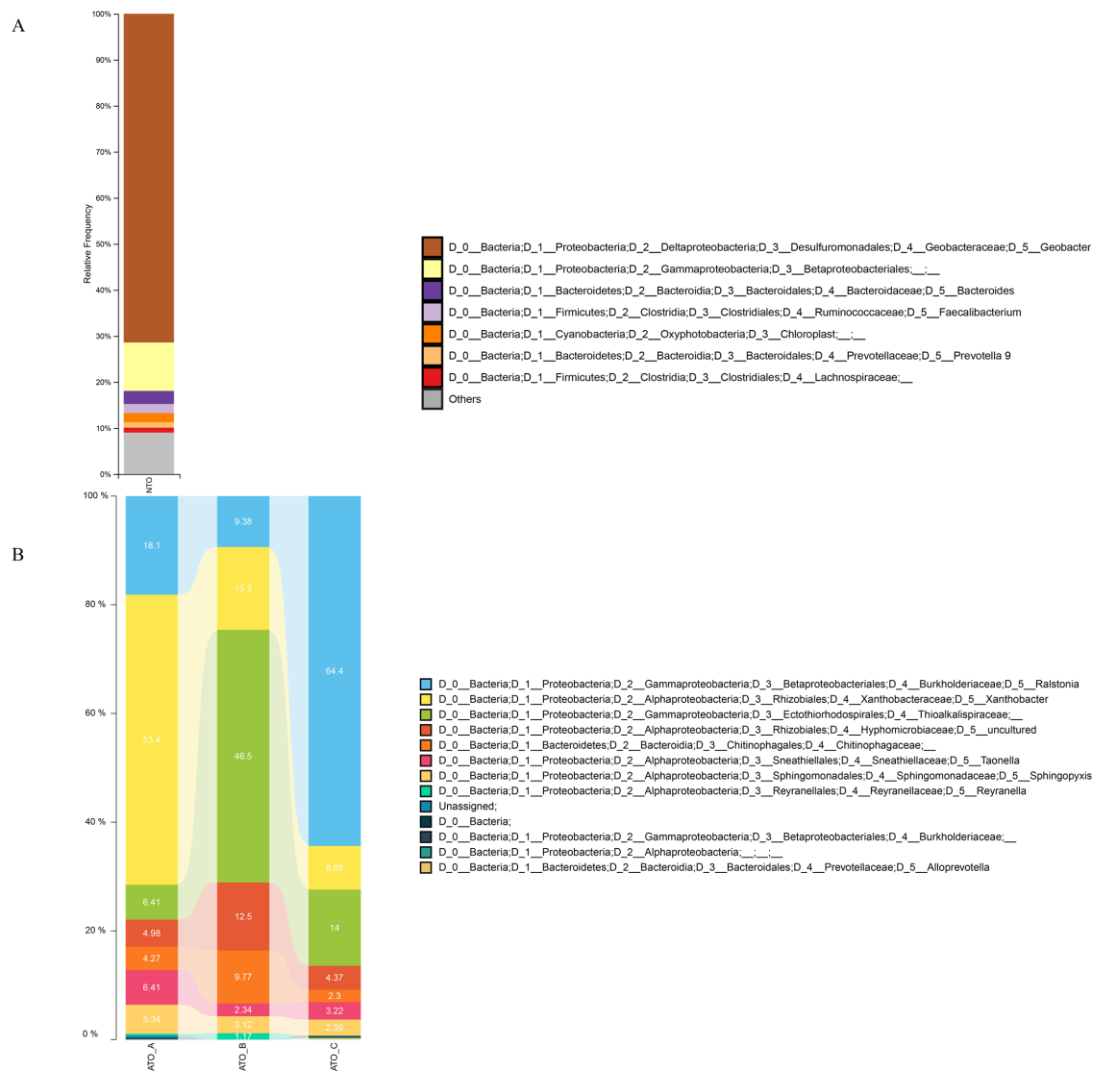


Figure 2 Relative abundance of 16S rRNA V4 region gene-based OTUs at the genus level. OTUs recovered from (A) the NTO metagenome and (B) the original ATO metagenomes were analyzed using the Qiime2 pipeline as described in detail in the Material and Methods section.

3.2 Recovery of metagenome-assembled genomes (MAGs)

To assess the community composition at the genome level and elucidate the total genetic potential of the consortia, population genome binning was performed with MaxBin 2.0 on the metagenomes of the NTO consortium and the three original ATO consortia and on a co-assembly of the 3 ATO metagenomes. Two MAGs were recovered in the NTO metagenome and seven MAGs in each ATO metagenome; eight MAGs were recovered based on the ATO co-assembly. The ATO MAGs were de-replicated using the genome-aggregate average nucleotide identity (ANI) at the 95% ANI level into eight MAGs. The pairwise ANI values of the MAGs assigned to the same genomospecies were all above 99.98% and the corresponding genome-aggregate amino acid identity (or AAI) values were above 99.23% as well. The quality of the MAGs was assessed based on the quality score from MiGA calculated as “completeness – 5 × contamination” estimated based on essential genes[27]. Except for two MAGs recovered from the ATO-A and ATO-B samples that showed low relative abundances, the quality of all the MAGs was high showing scores around 80.2 - 95.5 (Table 2).

Table 2 Summary statistics of MAGs recovered in this study. All assembled contigs from the metagenome longer than 500 bp were used for population genome binning with the MaxBin 2.0 algorithm. To taxonomically identify the MAGs, their genome sequences were searched against all available NCBI prokaryotic genomes using the MiGA, and the best matching NCBI genomes are shown on the 2nd column. The genome-aggregate average amino-acid identity (AAI) to the best matching NCBI genome is also reported on the 3rd column. Further statistics of the MAGs (e.g., N50, %GC) are also provided as well as the best match based on the 16S rRNA gene

Bin ID	Best Genome Match	AAI (%)	Comple.(%)	Contamin.	Quality Score	Total Length (bp)	N50	Best 16S rRNA gene	Identity (%)
NTO_MAG 1	<i>Geobacter anodireducens</i> NZ CP014963	98.31	100	1.9	90.5	3752065	118547	<i>Geobacter</i> sp. ^a	99.87
NTO_MAG 2	<i>Thauera humireducens</i> NZ CP014646	92.16	98.2	2.8	84.2	3847374	12019	<i>Salmonella</i> sp. ^a	75.27
ATO_MAG 1	<i>Xanthobacter autotrophicus</i> Py2 NC 009720	80.21	100	3	86	5724956	88216	<i>Xanthobacter</i> sp. ^b	99.74
ATO_MAG 2	<i>Sulfurivermis fontis</i> NZ AP018724	50.66	99.1	2.8	85.1	2881190	220830	Unclassified Gammaproteobacteria ^a	98.94
ATO_MAG 3	<i>Panacibacter ginsenosidivorans</i> NZ CP042435	55.62	98.1	0.9	93.6	5191604	419495	<i>Terrimonas</i> sp. ^a	97.25
ATO_MAG 4	<i>Hyphomicrobium nitrativorans</i> NL23 NC 022997	57.22	98.1	0.9	93.6	3610680	282239	<i>Hyphomicrobium</i> sp. ^b	99.49
ATO_MAG 5	<i>Ralstonia pickettii</i> 12D NC 012856	96.64	100	0.9	95.5	5250008	202495	<i>Ralstonia</i> sp. ^b	99.93
ATO_MAG 6	<i>Sphingopyxis terrae</i> subsp terrae NBRC 15098 CP013342	95.39	99.1	1.9	89.6	3913019	84938	<i>Sphingopyxis</i> sp. ^a	99.67
ATO_MAG 7	<i>Magnetospirillum</i> sp ME 1 NZ CP015848	50.35	100	2.8	86	7194355	86634	<i>Taonella</i> sp. ^b	100
ATO_MAG 8	<i>Magnetospirillum</i> sp ME 1 NZ CP015848	49.31	80.2	0	80.2	5477325	4904	<i>Reyranela</i> sp. ^a	99.86

^a16S rRNA gene recovered in MAGs. ^b 16S rRNA gene recovered in the contigs (not binned into MAGs).

3.3 NTO consortium

Similar to the 16S rRNA gene-based results, analysis of the NTO metagenome revealed only two MAGs accounting for almost the complete metagenome (94.82% of the relative abundance; Figure 3A, Table 2). The most abundant MAG (NTO_MAG1) constituted 89.29% of the total NTO consortium, followed by NTO_MAG2 that constituted 5.53% of the total. The relative abundances of these two MAGs were slightly higher than that of 16S rRNA gene v4 region OTUs assigned to the *Geobacter* genus and the *Betaproteobacteriales* order (81.9%). Taxonomic classification using MiGA showed that the closest described genome of the two MAGs was *Geobacter anodireducens* NZ_CP014963 with 98.31% AAI (same species assignment) and *Thauera humireducens* NZ_CP014646 with 92.16% of AAI (distinct but closely related species of the same genus). Thus, NTO_MAG1 and NTO_MAG2 likely represent members of the *G. anodireducens* species and *Thauera* genus, respectively, based on the most frequently used standards for species demarcation[42, 43].

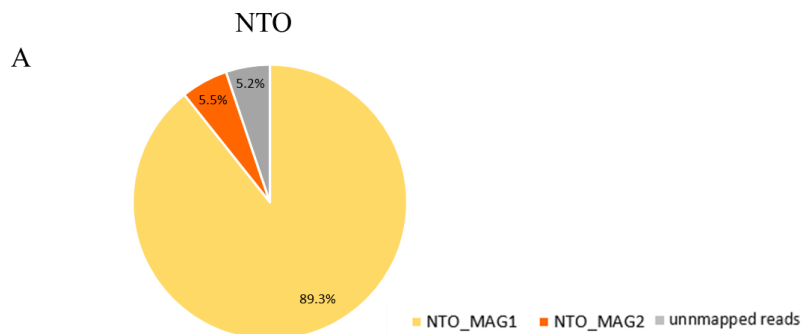


Figure 3A Composition of the NTO-reducing consortium. The relative abundance of recovered MAGs from the (A) NTO metagenome. The abundance was calculated by multiplying the genome size of the MAGs with their average sequence depth (coverage) and dividing the product by the total (sum) length of all trimmed reads of the metagenome (metagenome size). The predicted genome size of MAGs was obtained from the MiGA analysis. To get the average sequence coverage, TAD80 was obtained as described in the Material and Methods section.

3.4 Potential degradation of NTO in these MAGs

We hypothesized a nitroreductase might be responsible for the ATO reduction reaction because nitroreductases have been known to reduce similar nitroaromatic compounds including TNT, nitrofurazone, nitrobenzene, and even flavin[44]. Notably, both NTO_MAGs have genes related to or annotated as nitroreductases (Table 3). Five genes of NTO_MAG1 (*G. anodireducens*) show similarity, ranging from 30.1 to 36.2% amino acid identity, to the known nitroreductases of *Comamonas testosteroni*, *Leishmania infantum*, *Clostridium difficile*, *Bacillus megaterium*, *Vibrio harveyi*, and *Leishmania infantum*. Among these five genes, three genes (NTO_MAG1_2_47, 11_118, and 2_47) were also annotated as nitroreductase family genes by the RAST pipeline, indicating that these genes could be involved in the reduction of the nitro group. For NTO_MAG2 (*Thauera* sp.), four homologs were identified, showing amino acid identity ranging from 35.9 to 53.7% against experimentally verified nitroreductase genes from *Leishmania infantum*, *Bacillus megaterium*, *Pseudomonas oleovorans*, and *Mycobacterium smegmatis*. Two of the genes (MAG2_73_5, and MAG2_139_5) were also annotated as nitroreductases by the RAST pipeline. The matching, experimentally-verified nitroreductases from the public databases are known to govern reduction of nitro-compounds including chloronitrobenzene, nitro-drugs, mesotrione, and nitrobenzene[45-51].

Table 3. Candidate nitroreductases for NTO reduction to ATO and their experimentally verified best match homolog.

MAG	AA length (alignment)	Identity	Closest hit	Protein name	Accession	Responsible nitro-compound
NTO_MAG_15_126	80	36.2	<i>Comamonas testosteroni</i>	Chloronitrobenzene nitroreductase	Q5XW77	Chloronitrobenzene [49]
NTO_MAG1_2_88	216	34.3	<i>Leishmania infantum</i>	Nitroreductase	E9AGH7	Nitro-drugs (e.g. DNDIVL-2098) [45]
NTO_MAG1_11_118 ^a	160	33.8	<i>Clostridium difficile</i>	Nitroreductase	C9YJL7	Metronidazole [46]
NTO_MAG1_2_47 ^a	178	32	<i>Bacillus megaterium</i>	NADPH-dependent oxidoreductase	A0A0K0VJM8	Mesotrione [47]
NTO_MAG1_45_15 ^a	189	31.2	<i>Vibrio harveyi</i>	NADPH-flavin oxidoreductase	Q56691	p-nitroblue tetrazolium [51]

NTO_MAG1_3_106	229	30.1	<i>Leishmania infantum</i>	Nitroreductase	E9AGH7	Nitro-drugs (e.g. DNDIVL-2098)[45]
NTO_MAG2_25_1_1	216	53.7	<i>Leishmania infantum</i>	Nitroreductase	E9AGH7	Nitro-drugs (e.g. DNDIVL-2098) [45]
NTO_MAG2_19_6_7	120	47.5	<i>Leishmania infantum</i>	Nitroreductase	E9AGH7	Nitro-drugs (e.g. DNDIVL-2098) [45]
NTO_MAG2_73_5	252	39.3	<i>Bacillus megaterium</i>	NADPH-dependent oxidoreductase	A0A0K0VJM9	Mesotrione [47]
NTO_MAG2_13_9_5	220	39.5	<i>Pseudomonas oleovorans</i>	Nitrobenzene nitroreductase	Q6DLR9	Nitrobenzene [50]
NTO_MAG2_11_9_8	92	35.9	<i>Mycolicibacterium smegmatis</i>	Nitroreductase	A0R6D0	Benzothiazinones [48]

^aannotated as nitroreductase or nitroreductase family gene by RAST annotation

Since the reduction of nitro compounds by nitroreductase has been relatively well studied in bacteria, it might be more important to know what other proteins may interact with the nitroreductase. Interestingly, the most abundant MAG of the NTO consortium was assigned to the *Geobacter* genus, which has been extensively characterized for its extracellular electron transfer system (EET). The EET of NTO_MAG1 might be involved in NTO reduction by facilitating the transfer of electrons to the nitroreductase or other electron acceptors that could further reduce NTO to ATO. Thus, we evaluated the presence of EET systems encoded in the NTO_MAG1 genome by searching verified multi-heme cytochrome C proteins from *Geobacter* against the genome sequence (SI Table S1). Among 3429 ORFs, 3.4% of the total were identified as cytochromes and 54.8% of the cytochromes were multi-heme cytochromes. Most previously described proteins involved in EET were encoded in the NTO_MAG1 genome (SI Table S2). Specifically, two inner membrane-associated proteins participating in EET, annotated to be members of the MacA and CbcL families, were found. Three periplasmic associated EET proteins, PpcA, PpcD, and PpcE, were also identified. Additionally, nine ORFs of NTO_MAG1 were assigned to the outer membrane-associated Omc EET protein family, including three ORFs assigned to OmcS and two assigned to OmcZ.

3.5 Original ATO consortia

All seven (de-replicated) MAGs were present in all three ATO samples (A, B and C) and showed relatively high abundance in each (98.12%, 98.08%, and 94.96% of the total, respectively) (Table 2, Figure 3B) cumulatively accounting for almost the complete metagenome in each sample. However, the composition of the seven genomes was different among the samples, especially with respect to the most dominant genome in each consortium similar to the 16S rRNA gene-based data reported above. In cultures A and C, one genome represented almost half of their community (49.21% of the total for A, 44.63% of the total for C), while three genomes were relatively equally abundant in culture B compared to other two samples (Figure 3B). Taxonomic classification using the MiGA webserver showed that the most abundant genome in culture A was assigned to the *Xanthobacter autotrophicus* species, and the closest genome in the NCBI_prok database in MiGA was *X. autotrophicus* Py2 NC 009720 (with 80.21% of AAI; same genus assignment). The most abundant genome in culture C, ATO_MAG5 comprising 44.63% of the total culture C reads, however, was affiliated with the *Ralstonia* genus and the closest available genome was *R. pickettii* 12D NC 012856 (with 96.64% of AAI; same species assignment). Hence, ATO_MAG5 is likely a member of the *R. pickettii* species[42, 43]. Unlike these two consortia, the three most abundant genomes in consortium B, i.e., ATO_MAG2 (30.30%), ATO_MAG3 (21.22%), and ATO_MAG4 (18.66% of total culture B reads), were affiliated with the *Gammaproteobacteria* class, the *Chitinophagales* order, and the *Rhizobiales* order, respectively, with no lower classification available. The closest genomes to the ATO MAG2, MAG3 and MAG4, were *Sulfurivermis fontis* NZ AP018724 (with 50.66% of AAI), *Panacibacter ginsenosidivorans* NZ CP042435 (with

55.62% of AAI), and *Hyphomicrobium nitrativorans* NL23 NC 022997 (with 57.22% of AAI), respectively. Thus, these three MAGs likely represent novel species, if not genera, based on their AAI values. The other three MAGs that were relatively less abundant in all three samples were affiliated with the *Sphingopyxis terrae* species and two alphaproteobacterial classes.

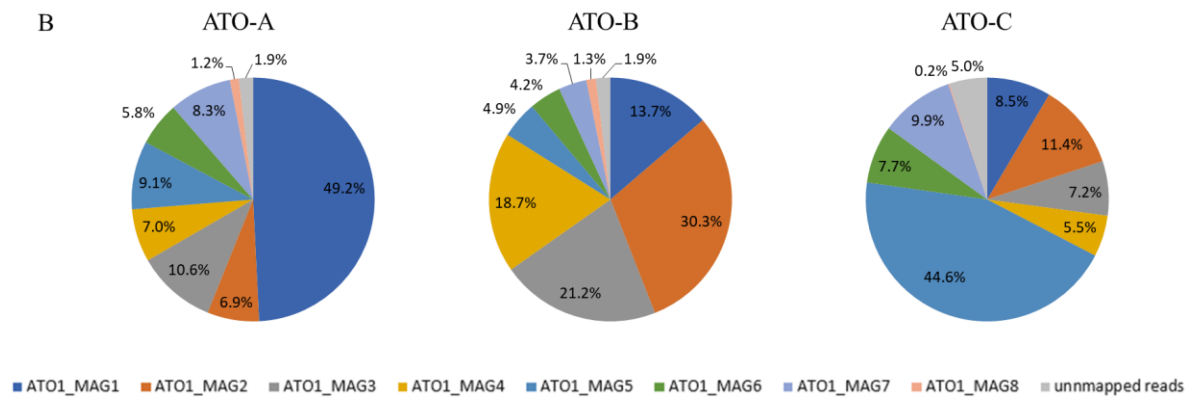


Figure 3B Composition of the original ATO-mineralization microbial consortia. The relative abundance of recovered MAGs.

Among the 8 ATO MAGs, four MAG sequences carried 16S rRNA gene sequences based on blastn matches (Table 2). Even though the 16S rRNA gene of ATO_MAG6 genome was only a partial match (1224 bp), the best match of all four of the MAGs against the RDP database agreed with their best whole-genome AAI-based classification by MiGA. The other four 16S rRNA genes of the MAGs were recovered based on correlation of the relative abundance of the 16S rRNA gene V4-based OTUs and the whole-genomes, and agreed with the best whole-genome AAI-based classification by MiGA as well. Hence, we

have been able to link all of the MAGs with their corresponding 16S genes via genome binning or correlation of abundances between V4-based OTUs and whole genomes.

We found fewer MAGs than the number of 16S rRNA gene-based OTUs extracted from the metagenomic reads but all MAGs recovered represented OTUs with highly congruent taxonomy; hence, the few 16S rRNA gene-based OTUs not represented by MAGs were apparently low-abundance (rare) members of the consortia. The relative abundance for the top five most abundant MAGs highly correlated with their corresponding OTUs with the same taxonomic assignment, showing a 0.999 ± 0.001 Pearson correlation coefficient.

3.6 Derived ATO consortia

In an attempt to further reduce the diversity of the consortium in order to narrow down the potential ATO degrader(s), we performed additional dilution to extinction (10^{-8} v/v) efforts with the culture B pretreated with EDTA and NaCl followed by separation of attached cells. This treatment attempted to eliminate extracellular polymeric substances that could adhere different cells together, including those cells not involved in ATO degradation. Sequencing of the four derived consortia revealed similar microbial composition to the original consortia with the exception of the ATO_MAG8 (closest to *Rhizobium* sp. N324 NZ CP013630) and ATO_MAG5 (closest to *Ralstonia pickettii* 12D NC 012856) abundance. Seven MAGs were still found in all four derived consortia (ATO-A2, B2, B2_EDTA, and B2_NaCl, Figure 3C) while ATO_MAG8 was eliminated from all samples and the abundance of ATO_MAG5 showed substantially lower (<1.22% of the

total in all derived consortia vs. 19.54%, on average, in the three original consortia). Also, while the composition of each MAG in these derived consortia differed slightly from the original consortia reported above, the distribution of 7 MAGs in these four consortia was generally similar to each other and to culture ATO-B. For instance, ATO_MAG1, ATO_MAG2, ATO_MAG3, and ATO_MAG4 were equally abundant in all four cultures, comprising about 84.17% of total metagenome reads.

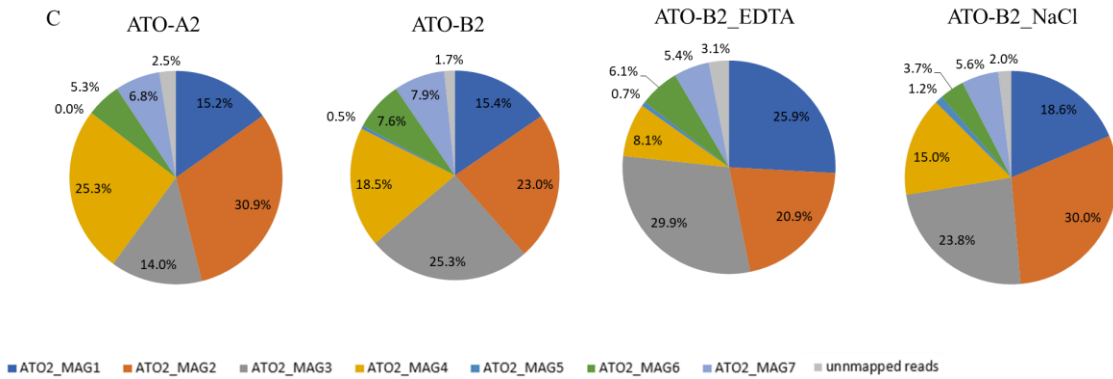


Figure 3C Composition of the derived ATO-mineralization microbial consortia. The relative abundance of recovered MAGs.

3.7 Prediction of functional dependence and interactions among members of the ATO consortium

We hypothesized that amino acid auxotrophies of the consortia may be the underlying reason(s) why the diversity of the ATO consortium was not reduced further after our efforts. To determine if this was the case, we first evaluated the amino acid synthesis pathways of each MAG. Because of the absence of ATO_MAG8 in the derived cultures and its relatively high genome incompleteness, we excluded this MAG from this analysis. Among 7 ATO MAGs, MAG1, MAG2, MAG3, and MAG5 showed one or more amino acid auxotrophies based on RAST and KAAS predictions (Figure 4A). In particular, MAG3 which was assigned to *Chitinophagales* order had the highest number of auxotrophies, showing a deficiency for four amino acid synthesis pathways (arginine, proline, serine, and lysine). The other three MAGs showed one amino acid auxotrophy each, i.e., asparagine for MAG1 and MAG5, threonine for MAG2. These results indicated that the amino acid auxotrophies might be one possible explanation for their tight association during our efforts to enrich the consortia for ATO degraders.

A

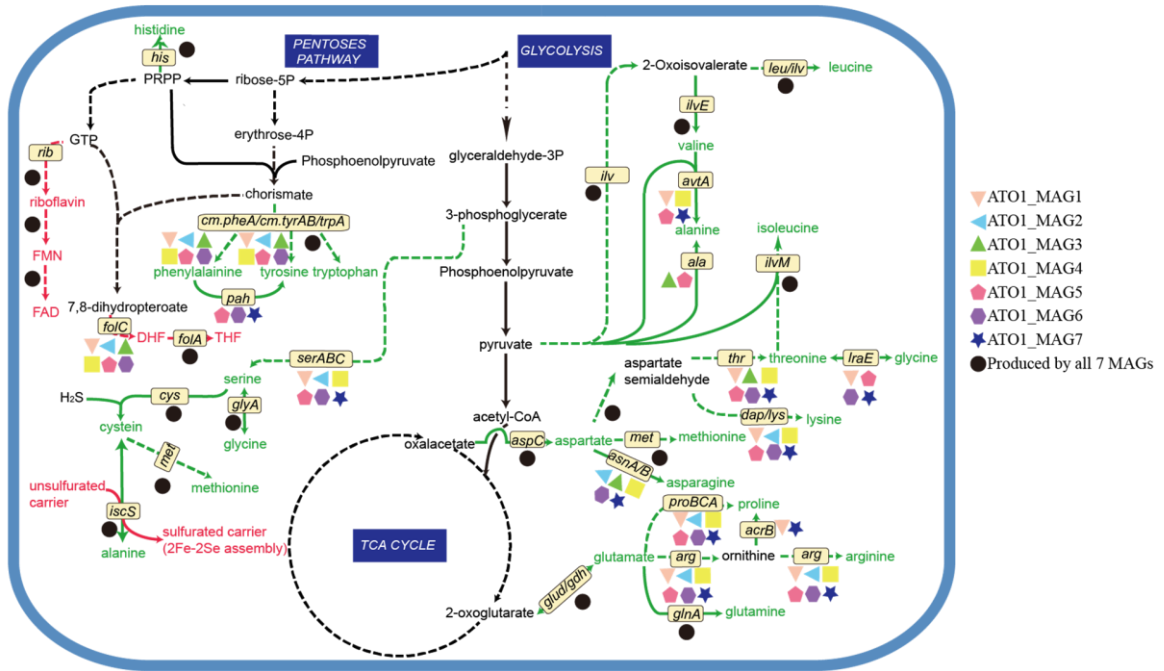


Figure 4 Prediction of functional dependencies and exchange of metabolites among MAGs of the ATO consortium. (A) Amino acid biosynthetic pathways found in the MAGs of the original ATO consortium (except for MAG8). Solid lines represent one reaction and the dashed lines represent two or more reactions.

To further assess interspecies interactions, especially the flux of metabolites, we simulated the growth of community compartmentalized models with the mineral media used in our culture (Figure 4B). Even though we could not completely mimic the physiological experiment due to the lack of information about the exact products of and underlying enzymes responsible for the ATO degradation, FBA showed that in addition to compounds that were exogenously added to the medium, each MAG interactively released and transported various metabolites through the cell. A total of 31 metabolites were transported in and out of the cells and these metabolites included organic carbon compounds, amino acids, inorganic nitrogen such as nitrite, nitrate and ammonium, and minerals, among others. Aside from the byproducts of aerobic growth (e.g., H₂O, CO₂, etc.), four amino acids showed active fluxes among cells. For example, a large quantity of aspartate was released by ATO_MAG4, and MAG5, which could be absorbed by MAG3 based on FBA analysis. Further, a large quantity of glutamate was also released by MAG2 and MAG3 and was likely taken up by MAG5. Moreover, a relatively minor flux of proline, lysine and 2-oxoglutarate was predicted between MAG4 and MAG5, which can be used as the materials for the synthesis of several amino acids. Interestingly, when we used minimal medium without any organic carbon (lactate) for FBA, fumarate, fructose, and glucose were predicted to be released outside the cell by MAG4, MAG5, and MAG7 respectively. In addition, several secondary metabolites including glucosamine, xanthine, trehalose were predicted to be exchanged among MAGs.

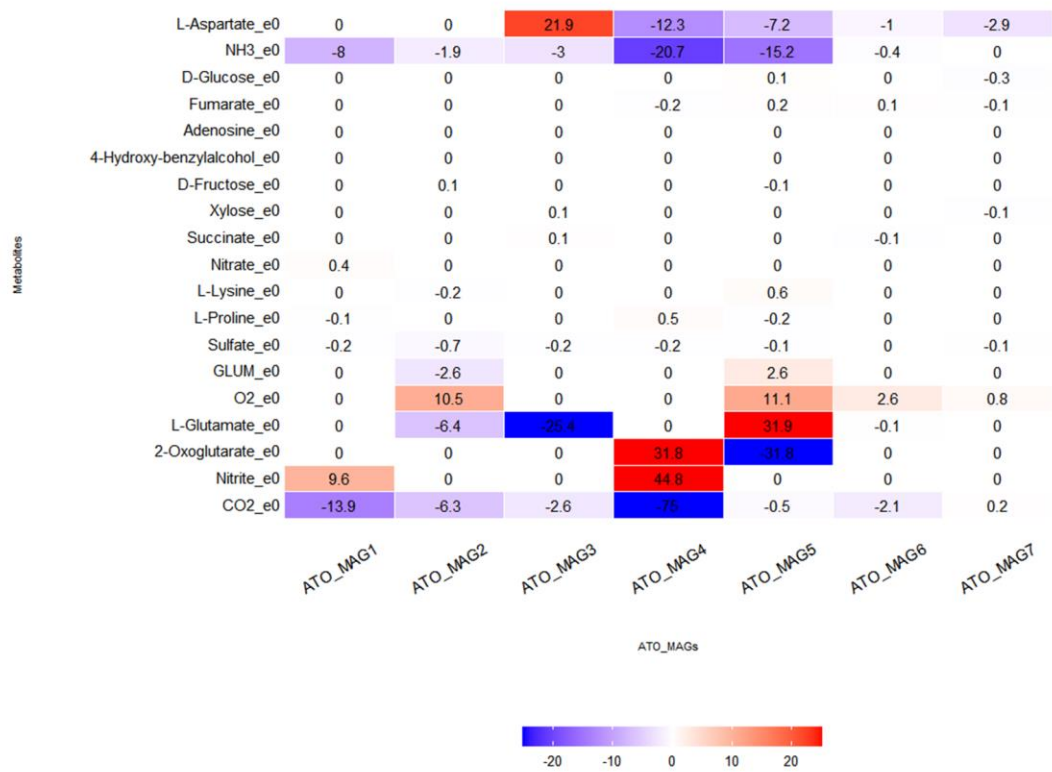


Figure 4 Prediction of functional dependencies and exchange of metabolites among MAGs of the ATO consortium. (B) The estimated metabolite fluxes for compartmentalized FBA model under mineral medium. Negative values represent releasing metabolites outside the cell and positive values represent uptake of metabolites into the cell.

CHAPTER 4. DISCUSSION

In this study, we provide near-complete genomic descriptions of NTO reduction enrichment cultures which produce ATO, and ATO biodegradation enrichment cultures which result in the full mineralization of ATO (Figure 5A). Bypassing the classical isolation approach, we obtained almost complete MAGs by sequencing enrichment cultures, and used these MAG sequences to predict genes potentially involved in NTO/ATO degradation. We compared ORFs from these MAGs against manually curated proteins with known function. Our metagenome analysis covered $98.5 \pm 1.2\%$ of the metagenomes indicating that no abundant member was missed by our sequencing effort (Figures 1 and 3). The abundant MAGs recovered in this study could provide information about key catabolic pathways as well as auxotrophies which might help guide future isolation work and NTO/ATO bioremediation efforts (Figure 4).

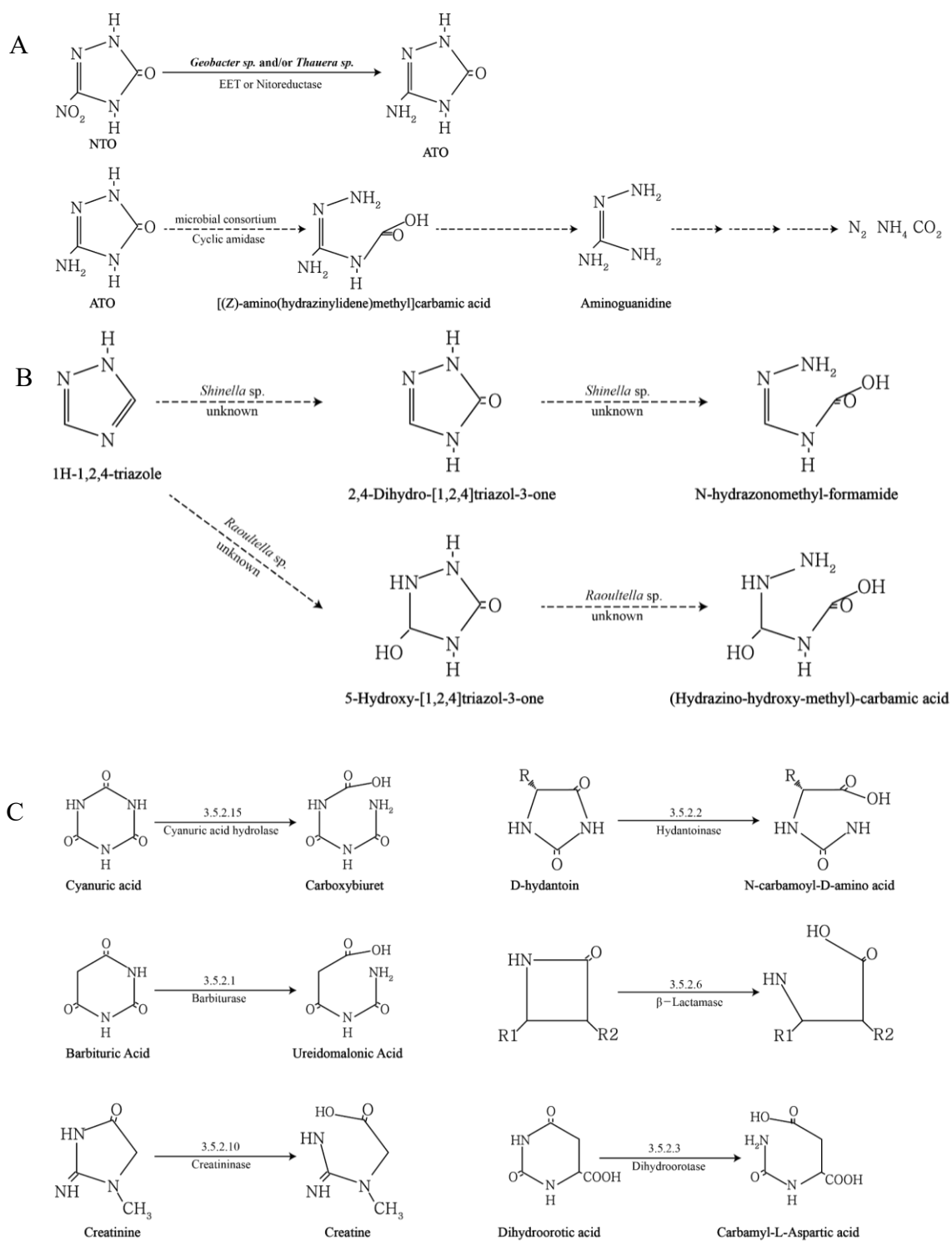


Figure 5 Proposed NTO degradation pathways. (A) the proposed NTO-ATO degradation pathways, (B) proposed 1H-1,2,4-triazol degradation pathways based on previous literature [1, 2], (C) known cyclic amidase reactions. The solid lines represent the previously described pathways and the dashed lines represent the proposed pathway herein.

Oxygen insensitive nitroreductase (type I) has been studied well and made up the majority of the nitroreductases. In particular, many of type I nitroreductases that have broad substrate specificity on a variety of nitro compound encompassing environmental pollutants, antimicrobial agents, and anticancer agents[52, 53] recovered in the MAGs sequences. A total of eleven nitroreductases homologs were recovered from the two NTO MAGs, albeit with relatively low amino acid sequence identity (ranging from 30.1 to 53.7%; Table 3) to previously described nitroreductases in the public databases. Despite the relatively low homology, these MAG candidate genes have the potential to catalyze NTO reduction based on several lines of evidence. For example, the nitroreductase of *Bacillus licheniformis*, showing only 28% of amino acid identity to that of *Escherichia coli*, can still reduce 5-Aziridinyl-2,4-dinitrobenzamide[54]. When clustering 24,270 nonredundant nitroreductases into 22 subgroups based on amino acid sequence similarities, the identities among members of the other subgroup typically range from ~ 35 to ~ 42% and the identities between any of the other subgroup members were ~ 27% [53]; thus this protein family shows extensive intra-family sequence divergence.

Further, the closest relatives of the MAGs, i.e., *Geobacter* sp. and *Thauera* sp. were previously shown to be able to reduce several nitro compounds[55, 56]. A previous study showed that the mixed culture of *Geobacter* sp. KT7 and *Thauera aromatica* KT9 cooperatively degrades 2-chloro-4-nitroaniline with an increased degradation rate compared to each species in isolation[55]. It was suggested that cross-feeding, nutrient sharing, and cooperation of the two species lead to increased degradation, although which enzymes contributed to the reduction of 2-chloro-4-nitroaniline have not yet been elucidated. Reduction of hexahydro-1,3,5-trinitro-1,3,5-triazine (RDX) can occur either by

direct electron transfer or indirect electron transfer as shown previously for *G. metallireducens*[56]. *Geobacter* species along with *Shewanella*, *Desulfovibrio*, and *Enterobacter* are well known electroactive bacteria (EAB)[57]. These EAB can release the electrons from intracellular reduction to the cell exterior that can then be utilized to reduce exogenous compounds. They can also obtain electrons from the anode in the bioelectrochemical system and consume the electrons for the reduction of an organic compound or intracellular metabolism[57], although the exact underlying proteins responsible remain unclear[57, 58]. Previous comparisons of six *Geobacter* EAB genomes showed that they contain an average of 79 cytochromes (2.1 % of the total proteins), a large fraction of which are multi-heme cytochromes[35]. Our *Geobacter* MAG (NTO_MAG1) carries a slightly higher number of single heme cytochromes but similar numbers of multi-heme cytochromes compared to previously described *Geobacter* sp. indicating that our MAG has the potential for an EET system (SI Table S1). Moreover, the specific cytochrome protein families used for EET including the PpcA, OmcBC, and CbcL families (SI Table S2) were found in our MAG. It is noticeable that MacA, also found in our MAG, functions in the transfer of electrons from the quinol pool to various periplasm cytochromes such as the CymA in *Shewanella oneidensis*[59]. The presence of EET systems in our MAG also makes possible the direct interspecies electron transfer (DIET) which has recently been observed between syntrophic growth organisms[60, 61]. Further studies should explore how these electron transfer mechanisms are involved in the function of the nitroreductases and in NTO reduction, and possible interactions with the *Thauera* MAG (NTO_MAG2) during co-culture.

The composition of consortia in the ATO enrichment cultures remained almost unchanged even after at least 55 transfers and three recent attempts to dilute to extinction. Previously, Madeira *et al.* showed 19 phylogenetic groups were present in this culture after 55 transfers and dilution to extinction[11]. However, after seven times more 10^{-3} dilution of the enrichment culture, only nine phylogenetic groups at almost equal abundances based on the quantitative PCR (qPCR) results survived and were present which is largely consistent with our metagenome-based results reported here (Figure 3B, C). However, among the phylogenetic groups not detected in the previous qPCR results, *Hyphomicrobium spp.* and *Xanthobacter spp.* were observed in our MAGs (MAG4 and MAG1 respectively). These two groups might have been present in the 10^{-7} diluted culture, but their abundance could have been low, and thus not detected by qPCR. According to our study, a total 7 MAGs of out of 8 MAGs survived the second dilution to extinction despite a physical treatment to separate cells (Figure 3C). Therefore, the overall consistent results from qPCR in Madeira *et al.* and MAG abundances as part of the present study indicate that co-metabolism or other strong interactions by the orchestrated activities of several distinct microorganisms are likely to occur when ATO is completely degraded to mineral $\text{NH}_4^+\text{-N}$, and N_2 , and CO_2 . In particular, the assessment of amino acid auxotrophies and the FBA results (Figure 4) provided preliminary evidence that several members of the consortium might actively exchange their metabolites. More accurate culture-simulation using FBA remains to be performed as revealed intermediates and genes corresponding to each step during the ATO degradation compared to what was performed here.

Notably, ATO degrading microorganisms in our enrichment cultures were distinct (novel) from previously described isolates based on their whole-genome AAI values (Table

2). Future work should focus on isolating these novel species and elucidating their exact functional role in ATO degradation. In the case of the ATO_MAG5 of which the closest genome revealed *Ralstonia picketti* 12D (96.64% AAI; same species), strain 12D is a well-known degrader of xenobiotics such as toluene, nitrobenzene, and trichloroethylene, and can live in oligotrophic environments[62, 63]. However, in the dilution to extinction (10^{-8} v/v) after treatment to separate cells, *R. picketti* MAG's abundance decreased dramatically suggesting that the reason why this was present might be due to its ability to survive in the oligotrophic environment (i.e., ATO was the sole carbon and nitrogen source) and/or grow on the extracellular polymer matrix. The possibility, however, that it is actively involved in ATO degradation cannot be excluded at present (Figure 4B). The other ATO MAG that closely matched a previously described strain, i.e., *Sphingopyxis terrae* NBRC15098 (95.39% AAI) was ATO_MAG6. Strain NBRC15098 was isolated from an activated sludge sample and has the ability to degrade polyethylene glycol (PEG)[64]. The *Sphingopyxis* genus is affiliated with the 'Sphingomonads', a collective group of several bacterial species known for the degradation of recalcitrant hydrophobic compounds such as lindane[65]. In addition to PEG and lindane, it has been reported that the one of the sphingomonad group species, can degrade pentachlorophenol (PCP)[66], a lignin-derived aromatic compound[67], and a wide range of aromatic hydrocarbon and heterocyclic compound[68]. It has been suggested that this catabolic versatility might be mediated by high genome plasticity and plasmid-borne gene transfer and recombination[65]. Unfortunately, it was not possible to identify candidate genes for ATO degradation by comparing these two genomes due to a plethora of uncharacterized gene functions and large gene content differences between our MAG and the *S. terrae* strain NBRC15098.

It has been challenging to identify the genetic determinants of ATO biodegradation due, at least in part, to the lack of axenic cultures. Many studies have been performed on isolates and enzymes that mediate the biodegradation of nitrogen heterocyclic compounds (NHCs). Two such studies found that 1H-1,2,4-triazole (TZ) that is widely used for the synthesis of pesticides and herbicides and is structurally similar to ATO can be degraded by *Shinella* sp. NJUST26[1] and *Raoultella* sp. NJUST42[2] (Figure 5B), but neither study identified the genes responsible for the biodegradation. de Souza *et al.* found that atrazine, one of the s-triazine herbicides, can be completely degraded by *Pseudomonas* sp. ADP, whose reaction was initiated by the AtzD enzyme, a member of cyclic amidases [69]. In addition to AtzD, many bacterial cyclic amidases can catalyze the hydrolytic ring-opening reaction of nitrogen heterocyclic compounds (Figure 5C) and we found several homologs of these enzymes in our MAGs that could be involved in the ATO ring-opening reaction or cleavage of the 1N-5C bond in the first step based on chemical structure similarity [1, 2, 70] (Figure 5C, Table 4). Most notably, MAG1 (*Xanthobacter* sp) has a homologous gene showing 83.9% amino acid identity to the experimentally verified cyanuric acid amidohydrolase (AtzD) of *Azorhizobium caulinodans*[71]. Besides starting off with ring opening reaction during the ATO degradation, the 3-amino group could be changed to a hydroxyl group or carbonyl group by a deaminase, followed by hydrolytic ring cleavage catalyzed by a cyclic amidase. This pathway has been proposed, for instance, to underlie the degradation of 1,2,4-triazole by Wu *et al.*[72].

Table 4 Candidate cyclic amide hydrolase for ATO degradation and their best match homolog

MAG	Gene		AA length (Alignment)	Identity (>50)	Closest hit	Accession	DB
Cyclic amidase							
ATO_MAG 1	<i>atzD</i>	Cyanuric acid amidohydrolyase	353	83.9	<i>Azorhizobium caulinodans</i>	A8IKD2	SwissProt
ATO_MAG 7	<i>Dht</i>	Hydantoinase	479	67.2	<i>Pseudomonas aeruginosa</i>	Q9I676	SwissProt
ATO_MAG 4	<i>blaP</i>	b-Lactamase	245	53.1	<i>Proteus mirabilis</i>	P30897	SwissProt
ATO_MAG 5	<i>pyrC</i>	Dihydroorotase	344	99.7	<i>Ralstonia pickettii</i>	B2UFJ8	SwissProt
ATO_MAG 6			340	91.2	<i>Sphingopyxis alaskensis</i>	Q1GT81	SwissProt
ATO_MAG 2			342	67.3	<i>Methylobacillus flagellatus</i>	Q1GYZ0	SwissProt
Other Cyclic amidase							
ATO_MAG 7	<i>crnA</i>	Creatininase	202	37.1	<i>Pseudomonas putida</i>	P83772	SwissProt
ATO_MAG 1			270	30.7	<i>Pseudomonas putida</i>	P83772	SwissProt

CHAPTER 5. CONCLUSIONS

Our metagenomic analysis suggests that two distinct clonal populations are involved in the NTO reduction to ATO. Notably, the most abundant MAG that is assigned to *Geobacter* species contains the conserved EET gene system, along with several putative nitroreductases, suggesting that NTO reduction might be associated with the transfers of electrons via the EET. In contrast to the two-population genome in NTO consortium very similar with the known genera, seven members were observed in the ATO consortia, even after repeated efforts to further reduce the diversity of the latter consortia by breaking up the extracellular matrix, and contained four (of a total of seven) novel genera. These findings and the genome sequences reported here should facilitate future efforts to identify the biodegradation genes and species-species interactions that underlie the biodegradation of NTO and ATO and, by extension, facilitate future bioremediation and monotonic efforts against these pollutants.

APPENDIX A. SUPPORTING INFORMATION

Table S1 *Geobacter* MAG cytochromes based on cytochrome annotation

	No in NTO_MAG1
ORFs in genome	3429
cytochromes total	115
cytochromes (% genome)	3.4
multi heme cytochromes	63
cytochromes (% multiheme)	54.8
hemes per cytochrome (average)	4.92

Table S2 Proposed *Geobacter* MAG EET (extracellular electron transfer system) based on cytochrome annotation

CytC Family ID ³⁰	Genetic code	Best hit gene description in NCBI	No. of ORFs in family	No. of CXXCH domain in NTO_MAG1 ORF	Estimated location
2568	macA family	cytochrome C peroxidase	1	2	Inner Membrane
1467	cbcL family	cytochrome C	1	9	Inner Membrane
49	ppcA family	cytochrome C3 family protein	1	3	Periplasm
3948	ppcD family	cytochrome C3 family protein	1	3	Periplasm
3353	ppcE family	cytochrome C3 family protein	1	3	Periplasm
1653	omcB family	C-type polyhemecytochrome OmcB	1	4	Outer Membrane
51	omaB family	cytochrome C	1	8	Periplasm/Outer Membrane
2177	omcE family	cytochrome C3 family protein	1	4	Outer Membrane
1292	omcQ family	cytochrome C3 family protein	1	12	Outer Membrane
64	omcS family	C-type cytochrome OmcS, hypothetical protein	3	6	Outer Membrane
2504	omcX family	cytochrome C	1	12	Outer Membrane
1253	omcY family	cytochrome C	1	8	Outer Membrane
2307	omcZ family	cytochrome C	2	7	Outer Membrane
1964	cbcA family	cytochrome C	1	7	Periplasm/Outer Membrane

Table S3 The composition of ATO minimal medium used in FBA

	Compounds	Concentrations	Minflux	Maxflux
Lactate ^a	cpd00159	0.001	-100	100
NH ₃	cpd00013	0.001	-100	100
H ₂ O	cpd00001	0.001	-100	100
O ₂	cpd00007	0.001	-100	100
CO ₂	cpd00011	0.001	-100	100
H ⁺	cpd00067	0.001	-100	100
Cl ⁻	cpd00099	0.001	-100	100
Na ⁺	cpd00971	0.001	-100	100
Phosphate	cpd00009	0.001	-100	100
K ⁺	cpd00205	0.001	-100	100
Ca ²⁺	cpd00063	0.001	-100	100
Sulfate	cpd00048	0.001	-100	100
Mg	cpd00254	0.001	-100	100
Boric acid	cpd09225	0.001	-100	0.1
Fe ²⁺	cpd10515	0.001	-100	0.1
Zn ²⁺	cpd00034	0.001	-100	0.1
Mn ²⁺	cpd00030	0.001	-100	0.1
Mo	cpd00131	0.001	-100	0.1
Co	cpd00149	0.001	-100	0.1
Ni	cpd00244	0.001	-100	0.1
Cu	cpd00058	0.001	-100	0.1

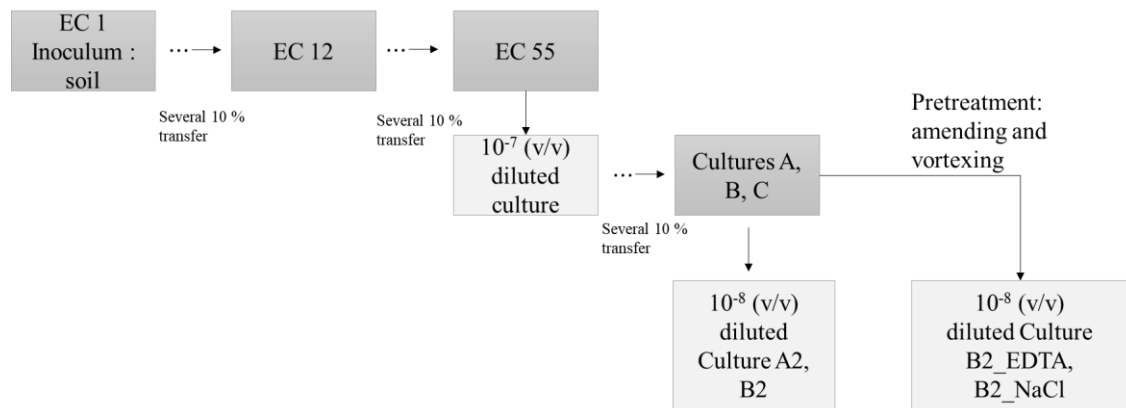


Figure S1 **Development of ATO enrichment cultures.**

REFERENCES

1. Wu, H., et al., *Biodegradation mechanism of 1H-1, 2, 4-triazole by a newly isolated strain Shinella sp. NJUST26*. Scientific reports, 2016. **6**: p. 29675.
2. Liu, X., et al., *1H-1, 2, 4-Triazole biodegradation by newly isolated Raoultella sp.: A novel biodegradation pathway*. Bioresource Technology Reports, 2019. **6**: p. 63-69.
3. Halasz, A., J. Hawari, and N.N. Perreault, *New insights into the photochemical degradation of the insensitive munition formulation IMX-101 in water*. Environmental science & technology, 2018. **52**(2): p. 589-596.
4. Dontsova, K., S. Taylor, and R. Pesce-Rodriguez, *Dissolution of NTO, DNAN and Insensitive Munitions Formulations and Their Fates in Soils*. 2018, University of Arizona Tuscon United States.
5. Pagoria, P., *A comparison of the structure, synthesis, and properties of insensitive energetic compounds*. Propellants, Explosives, Pyrotechnics, 2016. **41**(3): p. 452-469.
6. Taylor, S., et al., *Dissolution of three insensitive munitions formulations*. Chemosphere, 2015. **119**: p. 342-348.
7. Le Champion, L., et al., *Metabolism of 14C-Labelled 5-Nitro-1, 2, 4-Triazol-3-One by Rat Liver Microsomes Evidence for the Participation of Cytochrome P-450*. European journal of biochemistry, 1997. **248**(2): p. 401-406.
8. Le Champion, L., A. Vandais, and J. Ouazzani, *Microbial remediation of NTO in aqueous industrial wastes*. FEMS microbiology letters, 1999. **176**(1): p. 197-203.
9. Krzmarzick, M.J., et al., *Biotransformation and degradation of the insensitive munitions compound, 3-nitro-1, 2, 4-triazol-5-one, by soil bacterial communities*. Environmental Science & Technology, 2015. **49**(9): p. 5681-5688.
10. Madeira, C.L., et al., *Sequential anaerobic-aerobic biodegradation of emerging insensitive munitions compound 3-nitro-1, 2, 4-triazol-5-one (NTO)*. Chemosphere, 2017. **167**: p. 478-484.
11. Madeira, C.L., et al., *Microbial Enrichment Culture Responsible for the Complete Oxidative Biodegradation of 3-Amino-1,2,4-triazol-5-one (ATO), the Reduced Daughter Product of the Insensitive Munitions Compound 3-Nitro-1,2,4-triazol-5-one (NTO)*. Environmental Science & Technology, 2019. **53**(21): p. 12648-12656.

12. Rodriguez-R, L.M., et al., *How Much Do rRNA Gene Surveys Underestimate Extant Bacterial Diversity?* Applied and Environmental Microbiology, 2018. **84**(6): p. e00014-18.
13. Di Martino, P., *Extracellular polymeric substances, a key element in understanding biofilm phenotype.* AIMS microbiology, 2018. **4**(2): p. 274.
14. Tsementzi, D., et al., *Ecogenomic characterization of widespread, closely-related SAR11 clades of the freshwater genus "Candidatus Fonsibacter" and proposal of Ca. Fonsibacter lacus sp. nov.* Systematic and Applied Microbiology, 2019. **42**(4): p. 495-505.
15. Lo, C.-C. and P.S.G. Chain, *Rapid evaluation and quality control of next generation sequencing data with FaQCs.* BMC Bioinformatics, 2014. **15**(1): p. 366.
16. Peng, Y., et al., *IDBA-UD: a de novo assembler for single-cell and metagenomic sequencing data with highly uneven depth.* Bioinformatics, 2012. **28**(11): p. 1420-1428.
17. Rodriguez-R, L.M. and K.T. Konstantinidis, *The enveomics collection: a toolbox for specialized analyses of microbial genomes and metagenomes.* 2016, PeerJ Preprints.
18. Rodriguez-R, L.M., et al., *Nonpareil 3: Fast Estimation of Metagenomic Coverage and Sequence Diversity.* mSystems, 2018. **3**(3): p. e00039-18.
19. Johnston, E.R., et al., *Metagenomics reveals pervasive bacterial populations and reduced community diversity across the Alaska tundra ecosystem.* Frontiers in microbiology, 2016. **7**: p. 579.
20. McDonald, D., et al., *An improved Greengenes taxonomy with explicit ranks for ecological and evolutionary analyses of bacteria and archaea.* The ISME journal, 2012. **6**(3): p. 610.
21. Camacho, C., et al., *BLAST+: architecture and applications.* BMC bioinformatics, 2009. **10**(1): p. 421.
22. Altschul, S.F., et al., *Basic local alignment search tool.* Journal of Molecular Biology, 1990. **215**(3): p. 403-410.
23. Bolyen, E., et al., *Reproducible, interactive, scalable and extensible microbiome data science using QIIME 2.* Nature Biotechnology, 2019. **37**(8): p. 852-857.
24. Rognes, T., et al., *VSEARCH: a versatile open source tool for metagenomics.* PeerJ, 2016. **4**: p. e2584.

25. Quast, C., et al., *The SILVA ribosomal RNA gene database project: improved data processing and web-based tools*. Nucleic acids research, 2012. **41**(D1): p. D590-D596.
26. Wu, Y.-W., B.A. Simmons, and S.W. Singer, *MaxBin 2.0: an automated binning algorithm to recover genomes from multiple metagenomic datasets*. Bioinformatics, 2015. **32**(4): p. 605-607.
27. Rodriguez-R, L.M., et al., *The Microbial Genomes Atlas (MiGA) webserver: taxonomic and gene diversity analysis of Archaea and Bacteria at the whole genome level*. Nucleic acids research, 2018. **46**(W1): p. W282-W288.
28. Cole, J.R., et al., *Ribosomal Database Project: data and tools for high throughput rRNA analysis*. Nucleic acids research, 2014. **42**(Database issue): p. D633-D642.
29. Karthikeyan, S., et al., "*Candidatus Macondimonas diazotrophica*", a novel gammaproteobacterial genus dominating crude-oil-contaminated coastal sediments. The ISME Journal, 2019. **13**(8): p. 2129-2134.
30. Lagesen, K., et al., *RNAmmer: consistent and rapid annotation of ribosomal RNA genes*. Nucleic acids research, 2007. **35**(9): p. 3100-3108.
31. Consortium, T.U., *UniProt: a worldwide hub of protein knowledge*. Nucleic Acids Research, 2018. **47**(D1): p. D506-D515.
32. Buchfink, B., C. Xie, and D.H. Huson, *Fast and sensitive protein alignment using DIAMOND*. Nature methods, 2015. **12**(1): p. 59.
33. Ishii, S.i., et al., *Comparative metatranscriptomics reveals extracellular electron transfer pathways conferring microbial adaptivity to surface redox potential changes*. The ISME journal, 2018. **12**(12): p. 2844-2863.
34. Grant, C.E., T.L. Bailey, and W.S. Noble, *FIMO: scanning for occurrences of a given motif*. Bioinformatics, 2011. **27**(7): p. 1017-1018.
35. Butler, J.E., N.D. Young, and D.R. Lovley, *Evolution of electron transfer out of the cell: comparative genomics of six Geobacter genomes*. BMC genomics, 2010. **11**(1): p. 40.
36. Brettin, T., et al., *RASTtk: a modular and extensible implementation of the RAST algorithm for building custom annotation pipelines and annotating batches of genomes*. Scientific reports, 2015. **5**: p. 8365.
37. Henry, C.S., et al., *High-throughput generation, optimization and analysis of genome-scale metabolic models*. Nature biotechnology, 2010. **28**(9): p. 977.
38. Moriya, Y., et al., *KAAS: an automatic genome annotation and pathway reconstruction server*. Nucleic acids research, 2007. **35**(suppl_2): p. W182-W185.

39. Caspi, R., et al., *The MetaCyc database of metabolic pathways and enzymes*. Nucleic Acids Research, 2017. **46**(D1): p. D633-D639.
40. Arkin, A.P., et al., *KBase: The United States Department of Energy Systems Biology Knowledgebase*. Nature Biotechnology, 2018. **36**(7): p. 566-569.
41. Henry, C.S., et al., *Microbial Community Metabolic Modeling: A Community Data-Driven Network Reconstruction*. Journal of Cellular Physiology, 2016. **231**(11): p. 2339-2345.
42. Goris, J., et al., *DNA–DNA hybridization values and their relationship to whole-genome sequence similarities*. International journal of systematic and evolutionary microbiology, 2007. **57**(1): p. 81-91.
43. Jain, C., et al., *High throughput ANI analysis of 90K prokaryotic genomes reveals clear species boundaries*. Nature Communications, 2018. **9**(1): p. 5114.
44. Roldán, M.D., et al., *Reduction of polynitroaromatic compounds: the bacterial nitroreductases*. FEMS microbiology reviews, 2008. **32**(3): p. 474-500.
45. Wyllie, S., et al., *Activation of bicyclic nitro-drugs by a novel nitroreductase (NTR2) in Leishmania*. PLoS pathogens, 2016. **12**(11): p. e1005971.
46. Wang, B., et al., *Crystal structures of two nitroreductases from hypervirulent Clostridium difficile and functionally related interactions with the antibiotic metronidazole*. Nitric Oxide, 2016. **60**: p. 32-39.
47. Carles, L., et al., *Functional and structural characterization of two Bacillus megaterium nitroreductases biotransforming the herbicide mesotrione*. Biochemical Journal, 2016. **473**(10): p. 1443-1453.
48. Ribeiro, A.L.d.J.L., et al., *Analogous mechanisms of resistance to benzothiazinones and dinitrobenzamides in Mycobacterium smegmatis*. PloS one, 2011. **6**(11): p. e26675.
49. Wu, J.-f., et al., *Novel partial reductive pathway for 4-chloronitrobenzene and nitrobenzene degradation in Comamonas sp. strain CNB-1*. Applied and Environmental Microbiology, 2006. **72**(3): p. 1759-1765.
50. Somerville, C.C., S.F. Nishino, and J.C. Spain, *Purification and characterization of nitrobenzene nitroreductase from Pseudomonas pseudoalcaligenes JS45*. Journal of bacteriology, 1995. **177**(13): p. 3837-3842.
51. PARK, H.J., et al., *Purification and characterization of a NADH oxidase from the thermophile Thermus thermophilus HB8*. European journal of biochemistry, 1992. **205**(3): p. 881-885.

52. Rafii, F., G. Hehman, and A. Shahverdi, *Factors affecting nitroreductase activity in the biological reduction of nitro compounds*. *Current Enzyme Inhibition*, 2005. **1**(3): p. 223-230.
53. Akiva, E., et al., *Evolutionary and molecular foundations of multiple contemporary functions of the nitroreductase superfamily*. *Proceedings of the National Academy of Sciences*, 2017. **114**(45): p. E9549-E9558.
54. Emptage, C.D., et al., *Nitroreductase from Bacillus licheniformis: A stable enzyme for prodrug activation*. *Biochemical Pharmacology*, 2009. **77**(1): p. 21-29.
55. Duc, H.D., *Anaerobic degradation of 2-chloro-4-nitroaniline by Geobacter sp. KT7 and Thauera aromatica KT9*. *FEMS Microbiology Letters*, 2019. **366**(14).
56. Kwon, M.J. and K.T. Finneran, *Microbially Mediated Biodegradation of Hexahydro-1,3,5-Trinitro-1,3,5-Triazine by Extracellular Electron Shuttling Compounds*. *Applied and Environmental Microbiology*, 2006. **72**(9): p. 5933-5941.
57. Zhang, C.-L., et al., *Recent advances in nitroaromatic pollutants bioreduction by electroactive bacteria*. *Process biochemistry*, 2018. **70**: p. 129-135.
58. Yun, H., et al., *Polarity inversion of bioanode for biocathodic reduction of aromatic pollutants*. *Journal of hazardous materials*, 2017. **331**: p. 280-288.
59. Santos, T.C., et al., *Diving into the redox properties of Geobacter sulfurreducens cytochromes: a model for extracellular electron transfer*. *Dalton Transactions*, 2015. **44**(20): p. 9335-9344.
60. Shi, L., et al., *The roles of outer membrane cytochromes of Shewanella and Geobacter in extracellular electron transfer*. *Environmental microbiology reports*, 2009. **1**(4): p. 220-227.
61. Lovley, D.R., *Syntrophy goes electric: direct interspecies electron transfer*. *Annual review of microbiology*, 2017. **71**: p. 643-664.
62. Ryan, M.P., J.T. Pembroke, and C.C. Adley, *Ralstonia pickettii in environmental biotechnology: potential and applications*. *Journal of Applied Microbiology*, 2007. **103**(4): p. 754-764.
63. Monsieurs, P., et al., *Draft Genome Sequences of Ralstonia pickettii Strains SSH4 and CW2, Isolated from Space Equipment*. *Genome announcements*, 2014. **2**(5): p. e00887-14.
64. Ohtsubo, Y., et al., *Complete genome sequence of Sphingopyxis terrae strain 203-1 (NBRC 111660), a polyethylene glycol degrader*. *Genome Announc.*, 2016. **4**(3): p. e00530-16.

65. Nagata, Y., et al., *Lessons from the genomes of lindane-degrading sphingomonads*. Environmental Microbiology Reports, 2019. **11**(5): p. 630-644.
66. Copley, S.D., et al., *The Whole Genome Sequence of Sphingobium chlorophenolicum L-1: Insights into the Evolution of the Pentachlorophenol Degradation Pathway*. Genome Biology and Evolution, 2011. **4**(2): p. 184-198.
67. Masai, E., Y. Katayama, and M. Fukuda, *Genetic and biochemical investigations on bacterial catabolic pathways for lignin-derived aromatic compounds*. Bioscience, biotechnology, and biochemistry, 2007: p. 0612070214-0612070214.
68. Notomista, E., et al., *The marine isolate Novosphingobium sp. PPIY shows specific adaptation to use the aromatic fraction of fuels as the sole carbon and energy source*. Microbial ecology, 2011. **61**(3): p. 582-594.
69. de Souza, M.L., M.J. Sadowsky, and L.P. Wackett, *Atrazine chlorohydrolase from Pseudomonas sp. strain ADP: gene sequence, enzyme purification, and protein characterization*. Journal of bacteriology, 1996. **178**(16): p. 4894-4900.
70. Fruchey, I., et al., *On the Origins of Cyanuric Acid Hydrolase: Purification, Substrates, and Prevalence of AtzD from Pseudomonas sp. Strain ADP*. Applied and Environmental Microbiology, 2003. **69**(6): p. 3653-3657.
71. Seffernick, J.L., et al., *Defining sequence space and reaction products within the cyanuric acid hydrolase (AtzD)/barbiturase protein family*. Journal of bacteriology, 2012. **194**(17): p. 4579-4588.
72. Wu, H., et al., *Co-metabolic enhancement of 1H-1,2,4-triazole biodegradation through nitrification*. Bioresource Technology, 2019. **271**: p. 236-243.